 DOI: 10.1002/masy.201450401

Mechanical Properties of Magneto-Sensitive Elastomers in a Homogeneous Magnetic Field: Theory and Experiment

D. Ivaneyko,*[1,2] *V. Toshchevikov*,[1] *D. Borin*,[3] *M. Saphiannikova*,[1] *G. Heinrich*[1,2]

Summary: The aim of this study is to present a microscopic theory which describes the mechanical behaviour of magneto-sensitive elastomers (MSEs) under a uniform external magnetic field. For this we use a model where magnetic particles are located on the sites of the regular rectangular lattice. We introduce a structure parameter to describe isotropic, chain-like and plane-like particle distributions. Our theory is based on the equation for free energy as a function of strain. The magneto-induced deformation and the shear modulus are calculated as functions of the magnetization. It is shown that interaction between the magnetic particles results in the contraction of an elastomer along the homogeneous magnetic field. With increasing magnetic field the shear modulus for the shear deformation perpendicular to the magnetic field increases for all spatial distributions of magnetic particles. Furthermore, we have compared our result for the shear modulus to the experimental data and found good agreement.

Keywords: lattice models; magneto-sensitive elastomer; mechanical properties; microstructure; modelling; modulus

Introduction

Magneto-sensitive elastomers (MSEs), also known as magnetorheological elastomers, belong to a class of smart materials whose mechanical properties can be easily controlled by external magnetic fields.[1] Nowadays, MSEs have found a wide range of industrial applications in controllable membranes, rapid-response interfaces designed to optimize mechanical systems and in automobile applications such as adaptive tuned vibration absorbers, stiffness tunable mounts and automobile suspensions.[2,3]

MSEs consist of micron-sized iron particles dispersed within an elastomeric matrix. The particles are separated by the polymer matrix and are fixed in their average positions, since the size of magnetic particles used for synthesis of MSEs is much larger than the mesh size of an elastomeric matrix. Therefore, the particles cannot freely diffuse through the network.

The spatial distribution of magnetic particles in MSEs can be either isotropic or anisotropic[4] depending on whether the particles have been aligned by an applied magnetic field during the cross-linking of the polymer (see Figure 1). MSEs with isotropic distribution of magnetic particles are synthesized by cross-linking of a polymer melt with well-dispersed magnetic particles without any external field (Figure 1a). If the homogeneous magnetic field is applied to a polymer melt with magnetic particles, one obtains after the crosslinking the chain-like structures formed by the particles inside the MSE

[1] Leibniz-Institut für Polymerforschung Dresden e. V., Hohe Str. 6, 01069 Dresden, Germany
E-mail: ivaneiko@ipfdd.de
[2] Technische Universität Dresden, Institut für Werkstoffwissenschaft, Helmholtz Str. 7, 01069 Dresden, Germany
[3] Technische Universität Dresden, Institut für Strömungsmechanik, George-Bähr-Str. 3, 01069 Dresden, Germany

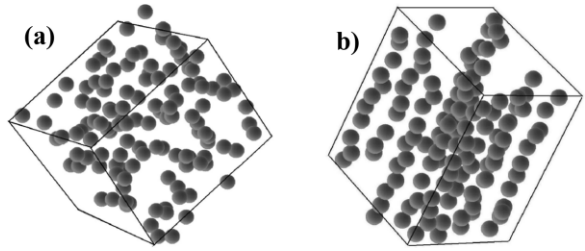

Figure 1.
Schematic presentation of MSE with isotropic (a) and chain-like (b) particle distribution.

(see Figure 1b).[1] Recently, the MSEs with plane-like spatial distributions of particles have been synthesized using the magnetic fields with rotating vector of the magnetic strength or under a strong shear flow before the cross-linking procedure.[5]

The magnetostriction effect and the change of the mechanical moduli are the most significant properties of the MSEs.[6] Under magnetostriction in the MSEs one understands the change of the MSE shape under the application of a magnetic field. Since the deformation of the MSEs can be either positive (elongation) or negative (contraction) in respect to the direction of applied external magnetic field, one distinguishes between positive and negative magnetostriction, respectively.

Magnetostriction of the MSEs has been a subject of extensive experimental,[6–11] analytical[12–18] and numerical[19–22] treatments. In theoretical studies of the mechanical behaviour of the MSEs, different analytical approaches were proposed, which can be divided into two groups: continuum-mechanics approach[14–18] and microscopic approach.[12,13] In the continuum-mechanics approach, the electromagnetic equations are coupled with the appropriate mechanical deformation equations and macroscopic homogeneity of magnetic media is assumed. This approach predicts a positive magnetostriction for MSEs (i.e. elongation along the external magnetic field).[14,15,18] The results of the continuum-mechanics approach are in agreement with experiments,[4,18] which show that MSEs with homogeneous distribution of magnetic particles demonstrate a uniaxial expansion along the magnetic field. On the other side, it was shown experimentally,[4,8,23] that MSEs with chain-like distributions of magnetic particles demonstrate a uniaxial contraction along the magnetic field. Uniaxial contraction of MSEs was demonstrated theoretically using the microscopic approaches which take the discrete distribution of magnetic particles explicitly into account.[12,13,24,25] Thus, the use of different theoretical approaches is very promising for understanding the microscopic processes which take place in MSEs under influence of magnetic fields.

Another important topic is the influence of the magnetic field on the mechanical moduli of MSEs. Many experimental works studied the dependence of the static mechanical moduli of MSE on the magnitude of external magnetic field.[10,26–36] The experimental works show that the static shear moduli of MSEs increase with increasing strength of the magnetic field and depend on the microstructure of these materials, e.g., on the volume fraction and spatial distribution of magnetic particles.[27]

Theoretical study of the static moduli of MSEs in a homogeneous magnetic field is a more complicated problem as compared to studies of magnetostriction effect. Only a few works have been proposed to calculate the static moduli of MSEs. These works used microscopic approaches taking into account a discrete distribution of magnetic particles. Here, we can mention a phenomenological approach,[37] one-chain discrete model called quasi-static one dimensional model,[12,23,38] multi-chain discrete model[39] and the lattice model[24,25] developed recently

by us to study the mechanical moduli of MSEs with homogeneous, chain-like and plan-like distributions of magnetic particles.

The main aim of the present work is to extend our previous theory[24,25] and to calculate the shear modulus of MSEs, taking into account the possible large magneto-induced deformation. The results of our theory are compared with experimental data.

Lattice Model and the Free Energy of an MSE

To simulate an MSE with isotropic and anisotropic spatial distributions of magnetic particles in the frame of a microscopic approach we introduce a lattice model (see Figure 2a). In this model, it is assumed for simplicity that spherical magnetic particles of the radius r are located at the sites of a regular rectangular lattice.

In the absence of an external magnetic field, the distances between neighbouring particles along the x-, y- and z-axes are $L_x^{(0)}$, $L_y^{(0)}$ and $L_z^{(0)}$, respectively. We assume that the distance $L_x^{(0)}$ can differ from the distances $L_y^{(0)}$ and $L_z^{(0)}$: $L_x^{(0)} \neq L_y^{(0)} = L_z^{(0)}$. Furthermore, we introduce a dimensionless structure parameter $\alpha = L_x^{(0)}/L_y^{(0)}$ in order to describe different spatial distributions of magnetic particles in a polymer matrix: isotropic distribution ($\alpha = 1$), chain-like distribution ($\alpha < 1$) and plane-like distribution ($\alpha > 1$), see Figure 3. Under such assumption, the x-axis is the axis of symmetry of an MSE: it lies along the chains in the chain-like structures and is perpendicular to the planes formed by the magnetic particles in the plane-like structures. The volume fraction of the particles, ϕ, is estimated as $\phi = \upsilon_0/(L_x^{(0)} L_y^{(0)} L_z^{(0)})$, where $\upsilon_0 = 4\pi r^3/3$ is the volume of a magnetic particle.

To describe chain-like and plane-like distributions of magnetic particles in real MSEs we choose the values of the structure

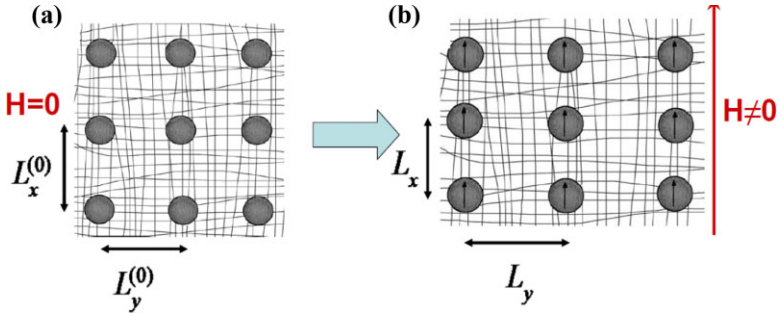

Figure 2.
A model of an MSE with magnetic particles arranged on the sites of a regular rectangular lattice, when (a) the external magnetic field **H** is turned off, or (b) the external magnetic field **H** is turned on.

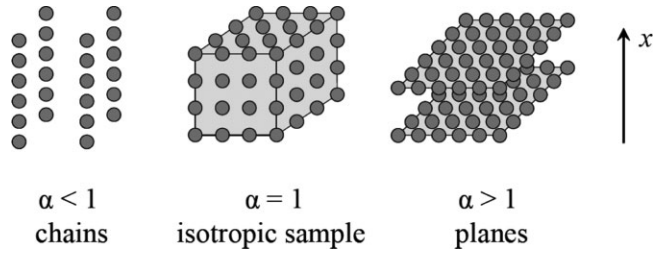

Figure 3.
Three different spatial distributions of magnetic particles inside an MSE.

parameter α in such a way, that the initial gap between nearest particles equals the radius of a particle r. Then the distance between particles in the chain-like structures is $L_x^{(0)} = 3r$. This gives for the chain-like structures:

$$\alpha_{ch} = \sqrt{\frac{81\phi}{4\pi}}. \quad (1)$$

For the plane-like structures the distance between nearest particles has been chosen as $L_y^{(0)} = 3r$, which corresponds to the value of α:

$$\alpha_{pl} = \frac{4\pi}{81\phi}. \quad (2)$$

Note, that it was shown experimentally that the chain-like structures contain gaps between particles, these gaps being of the order of the size of particles.[8,19]

Application of a magnetic field induces a magnetic moment in each particle along the direction of the field. In our work we consider such a configuration when the magnetic field is directed along the axis of symmetry (x-axis in Figure 3). Interaction between the induced magnetic moments of the particles leads to pair-wise attraction and repulsion of the magnetic particles depending on their mutual positions. This interaction results in a shape change of an MSE.

In order to relate displacements of particles with the macroscopic deformation we use the approximation of affinity of deformation,[40,41] which can be written as:

$$\left(R_{ij}\right)_x = \left(R_{ij}^0\right)_x \lambda_x = \left(R_{ij}^0\right)_x \lambda, \quad (3)$$

$$\left(R_{ij}\right)_y = \left(R_{ij}^0\right)_y \lambda_y = \left(R_{ij}^0\right)_y \lambda^{-1/2}, \quad (4)$$

$$\left(R_{ij}\right)_z = \left(R_{ij}^0\right)_z \lambda_z = \left(R_{ij}^0\right)_z \lambda^{-1/2}, \quad (5)$$

where $\left(R_{ij}\right)_\xi$ and $\left(R_{ij}^0\right)_\xi$ are the components of vectors, that separate two magnetic particles after and before deformation, respectively, ($\xi = x, y, z$). Here λ is the relative elongation of the sample along the x-axis. Equations (3)-(5) take into account the condition of constant volume for elastomers.[40,41]

The condition of affinity of deformation means that the displacements of particles are assumed to be a single-valued function of the elongation ratio λ and does not depend on the magnetic field in an explicit form. Under such approach the free energy of a deformed sample under magnetic field is written in the form:

$$F = F_{el} + F_m, \quad (6)$$

where the first part F_{el} is the elastic energy due to the entropic elasticity of polymer chains. Since under affine deformation the displacements of particles are independent of the magnetic field and the polymer chains are non-magnetic, the contribution F_{el} does not depend on the magnetic field in an explicit form and is a function only of the elongation ratio λ: $F_{el} = F_{el}(\lambda)$. In the case of non-linear deformation of an incompressible MSE, the elastic free energy per unit volume can be expressed through the Neo-Hooke law:[42]

$$F_{el} = \frac{G_0}{2}\left(\lambda^2 + \frac{2}{\lambda} - 3\right) \quad (7)$$

where the material parameter G_0 is the shear modulus of a filled polymer matrix.

The second part F_m of the free energy in equation (6) arises from the potential energy of magnetic particles placed in an external magnetic field and consists of the sum of the dipole-dipole interaction energy and the dipole-field interaction energy. The derivation of the function F_m is given in the Appendix, its expression can be presented in the following form:

$$F_m = -\mu_0 \frac{N}{V}(\mathbf{m}_i \cdot \mathbf{H}) - \frac{1}{V}\frac{\mu_r \mu_0}{4\pi} \times \sum_{ij}\left[\frac{3(\mathbf{m}_i \cdot \mathbf{R}_{ij})(\mathbf{m}_j \cdot \mathbf{R}_{ij})}{|\mathbf{R}_{ij}|^5} - \frac{(\mathbf{m}_i \cdot \mathbf{m}_j)}{|\mathbf{R}_{ij}|^3}\right]. \quad (8)$$

Here μ_0 is the permeability of the vacuum, V is the volume of the sample, N is the number of particles, μ_r is the relative permeability of the medium. In the present

work we consider an elastomeric matrix to be non-magnetic, therefore everywhere below we set $\mu_r = 1$. Here $\mathbf{m}_i$ and $\mathbf{m}_j$ are dipole moments of i-th and j-th magnetic particles, $\mathbf{R}_{ij}$ is the radius vector that joins the i-th and j-th magnetic particles. $\mathbf{H}$ is the external magnetic field. In our theory we assume all particles to be of the same size and magnetic properties. It means that magnetic dipoles $\mathbf{m}_i$ and $\mathbf{m}_j$ are equal to $\mathbf{m}$ and can be expressed via magnetization of the particles $\mathbf{M}$: $\mathbf{m} = \mathbf{M}\, v_0$.

Substituting equations (3)-(5) into (8) and taking into account that the dipole-field interaction energy $-\mu_0 \frac{N}{V}(\mathbf{m}_i \cdot \mathbf{H})$ is independent of the elongation ratio λ, since the magnetic dipoles of the particles $\mathbf{m}_i$ are assumed to be independent of the elongation ratio λ, we get the magnetic free energy in a form:[24,25]

$$F_m = -\frac{\mu_0}{4\pi}\phi^2 M^2 f_0(\alpha, \lambda). \tag{9}$$

Note, that F_m in equation (9) depends on ϕ and $\mathbf{M}$ through their combination $\phi\mathbf{M}$, which is a magnetization of the sample: $\mathbf{M}_r = \phi\mathbf{M}$. Function $f_0(\alpha, \lambda)$ is the dimensionless function of the structure parameter α and λ:

$$f_0(\alpha, \lambda) = \alpha\lambda^{\frac{3}{2}} \sum_{\{i_x i_y i_z\}\neq 0} \frac{2\alpha^2\lambda^3 i_x^2 - i_y^2 - i_z^2}{\left[\alpha^2\lambda^3 i_x^2 + i_y^2 + i_z^2\right]^{\frac{5}{2}}}. \tag{10}$$

Here the sum runs over all sites of the regular rectangular lattice, excluding the point $i_x = i_y = i_z = 0$.

In next section we study the magnetostriction effect occurred in MSEs under external magnetic field and estimate the quantitative values depending on the material parameter G_0, structure parameter α and magnetization of the sample $\mathbf{M}_r$.

Magnetostriction Effect

Pair-wise interaction between the magnetic moments of particles leads to the attraction and repulsion of the magnetic particles depending on their mutual positions. This behavior of the particles leads to elastic response of the matrix. In the absence of other mechanical loading on the MSE, the sample tends to achieve the equilibrium state, which is characterized by the equilibrium elongation λ_{eq}. To obtain an equation for the equilibrium elongation λ_{eq} of the sample, we minimize the free energy with respect to the elongation ratio λ at the constant value of $\mathbf{M}_r$:

$$\left.\frac{\partial F}{\partial \lambda}\right|_{M_r = const} = 0. \tag{11}$$

Using equations (7) and (9), the equation (11) for the equilibrium elongation λ_{eq} can be rewritten as follows:

$$G_0\left(\lambda_{eq} - \frac{1}{\lambda_{eq}^2}\right) + \frac{\mu_0}{4\pi} M_r^2 f(\alpha, \lambda_{eq}) = 0. \tag{12}$$

Note, that λ_{eq} depends on $\mathbf{M}_r$, G_0 and μ_0 through the dimensionless parameter $\frac{\mu_0}{4\pi G_0} M_r^2$. The function $f(\alpha, \lambda_{eq})$ is the dimensionless function of α and λ_{eq}:

$$f(\alpha, \lambda_{eq}) = \alpha\sqrt{\lambda_{eq}} \times \sum_{\{i_x i_y i_z\}\neq 0} \frac{12\alpha^4\lambda_{eq}^6 i_x^4 - 30\alpha^2\lambda_{eq}^3 i_x^2\left(i_y^2 + i_z^2\right) + 3\left(i_y^2 + i_z^2\right)^2}{2\left[\alpha^2\lambda_{eq}^3 i_x^2 + i_y^2 + i_z^2\right]^{\frac{7}{2}}}. \tag{13}$$

The transcendental equation (12) we solve numerically. Results are shown in Figure 4, where we present the equilibrium elongation

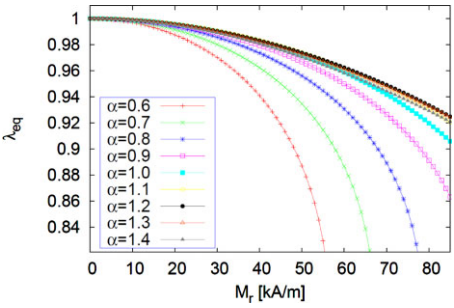

Figure 4.
Dependence of the equilibrium elongation λ_{eq} on the magnetization $\mathbf{M}_r$ at different values of the structure parameter α and at fixed value of $G_0 = 37.5$ kPa.

λ_{eq} as a function of the sample magnetization $\mathbf{M}_r$ at different α. The material parameter G_0 was chosen to be equal to 37.5 kPa. This value has been found in the experiment discussed below in section **Discussion**.

As one can see from Figure 4, our approach predicts a uniaxial contraction of MSEs along the magnetic field for all structures: isotropic, chain-like and plane-like. This result is in a good agreement with experimental data for MSEs with chain-like distribution of magnetic particles.[43] Furthermore, one can see from Figure 4 that at fixed value of $\mathbf{M}_r$ the magnitude of deformation $|\lambda_{eq} - 1|$ decreases at increasing value of the structure parameter α. This means that the magnetic response becomes smaller than the elastic response at higher values of α. Note, that the increasing of α means a transformation from the chainlike ($\alpha < 1$) to the plane-like ($\alpha > 1$) structure via isotropic one ($\alpha = 1$).

The change of the free energy of an MSE, ΔF, after small shear displacement $(\Delta R_{ij})_z$ from the equilibrium state (with $\lambda = \lambda_{eq}$) can be written as:

$$\Delta F = \frac{G_0 \gamma^2}{2} + \Delta F_m(\gamma, \lambda_{eq}). \quad (17)$$

Here $\Delta F_m(\gamma, \lambda_{eq})$ is the change of the magnetic energy after the shear displacement from the equilibrium state:

$$\Delta F_m(\gamma, \lambda_{eq}) = F_m(\gamma, \lambda_{eq}) - F_m(\lambda_{eq}). \quad (18)$$

In ref.[24] we have calculated the free energy ΔF as a function of γ using equations (14)–(16) as well as the shear modulus determined as $G = (\partial^2 \Delta F/\partial \gamma^2)_{\gamma=0}$. We have obtained the value G in the form:[24]

$$G = G_0 + \frac{\mu_0}{4\pi} M_r^2 f_3(\alpha, \lambda_{eq}), \quad (19)$$

where $f_3(\alpha, \lambda_{eq})$ is a dimensionless function:

$$f_3(\alpha, \lambda_{eq}) = 3\alpha^3 \lambda_{eq}^{\frac{9}{2}} \sum_{\{i_x i_y i_z\} \neq 0} \frac{i_x^2 \left[4\alpha^4 \lambda_{eq}^6 i_x^4 + 3\alpha^2 \lambda_{eq}^3 i_x^2 \left(i_y^2 - 9 i_z^2\right) - i_y^4 + 3 i_y^2 i_z^2 + 4 i_z^4\right]}{\left[\alpha^2 \lambda_{eq}^3 i_x^2 + i_y^2 + i_z^2\right]^{\frac{9}{2}}}. \quad (20)$$

The Shear Modulus

To study the static shear modulus we have considered a shear deformation applied to an MSE perpendicular to the magnetic field, i.e. it is applied along the z-axis. The shear strain is given by $\gamma = \Delta(R_{ij})_z/(R_{ij})_x$, where $\Delta(R_{ij})_z$ denotes the displacement of a particle in z direction. The new coordinates of the particles in the elastomer under both magnetic field and shear deformation are given by the following equations:

$$(R_{ij})_x = \left(R_{ij}^0\right)_x \lambda_{eq}. \quad (14)$$

$$(R_{ij})_y = \left(R_{ij}^0\right)_y \lambda_{eq}^{-1/2}, \quad (15)$$

$$(R_{ij})_z = \left(R_{ij}^0\right)_z \lambda_{eq}^{-1/2} + \gamma \left(R_{ij}^0\right)_x \lambda_{eq}. \quad (16)$$

Here $\left(R_{ij}^0\right)_\xi$ are the components of vectors that separate i-th and j-th particle in the absence of any fields.

From equation (19) one can see that the modulus G is an even function of the magnetization $\mathbf{M}_r$, since the value λ_{eq} is an even function of $\mathbf{M}_r$, according to equation (12). The shear modulus increases at increasing magnetization for all distributions of magnetic particles (see Figure 5). This tendency is in agreement with experimental data.[10] Moreover, the dependence of G on the magnetization is very sensitive to the spatial distribution of magnetic particles: the value of G increases with increasing $\mathbf{M}_r$ only slightly for the isotropic ($\alpha = 1$) and plane-like ($\alpha > 1$) distributions of magnetic particles, as compared with the chain-like ($\alpha < 1$) distributions. This can be explained by especially strong magnetic interactions between particles in the chain-like structures. The total force of these pair-wise interactions is directed along the axis of chain, which makes this type of structure

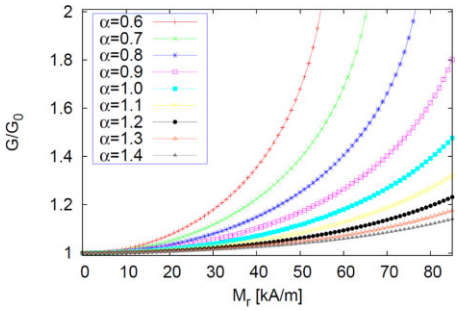

Figure 5.
Dependence of the shear modulus G on the magnetization $\mathbf{M}_r$ at different values of the structure parameter α and at fixed value of $G_o = 37.5$ kPa.

strongly resistant against the shearing perpendicular to the chains.

Experiment Part

Experimental characterisation of the MSE under oscillating shear loading has been done in order to perform a quantitative proof of the proposed model. The samples of MSE have been synthesized within the common procedure[11,20] using low molecular vinyl-containing rubber as a matrix, which has been polymerized at 150 °C. As a powder the particles of FeNdBr with an average diameter of ~35 μm with a concentration of ~30 vol. % were used. The material of the powder is magnetic hard and due to that the MSE being once magnetized in the external field remains its magnetization after the field is switched off, like the permanent magnet. Furthermore, due to the remanent magnetization the behaviour of such MSE will be similar to one of MSE with magnetic soft filler under the field influence. As far as the remanent magnetization of the sample is known, it is possible to proof the theoretical model using real experimental data.

Magnetic Properties

The movements of the particles of the filler are partially restricted due to the elasticity of the matrix. Due to this fact the character of the magnetization curve, as well as the remanent magnetization of the MSE should differ from that of the particles not embedded into the matrix. Magnetic measurements have been performed using a vibration sample magnetometer VSM 7400 (Lake Shore, USA). In Figure 6 the whole magnetization curve of the MSE with magnetic hard filler is presented.

The form of the curve is typical for the magnetic hard material. Initially particles are not magnetized and the virgin curve (1) is observed. Decreasing (2) of the applied field $\mathbf{B}$, after the saturation magnetization has been reached, will lead to the appearance of the remanent magnetization $\mathbf{M}_r$. Further decreasing of the field leads to the appearance of the coercitive force $\mathbf{H}_{c1}$, where an intensity of the external field is calculated as $\mathbf{H} = \mathbf{B}/\mu_0$. After the saturation for the negative field direction was reached, the back curve (3) is measured and the coercitive force $\mathbf{H}_{c2}$ is observed. The interesting fact is that the shape of the back curve (3) and therefore a value of the $\mathbf{H}_{c2}$ depends on the number of the magnetization cycles, but it is out of importance here, since it has no any influence on the remanent magnetization. Thus, analogous to the bulk magnetic hard material the virgin sample of the elastic composite can be magnetized in order to obtain a certain value of the magnetization $\mathbf{M}_r$. The dependence of $\mathbf{M}_r$ as a function of the field with a flux density $\mathbf{B}$, which has been applied to the sample for its magnetization, is shown in Figure 7.

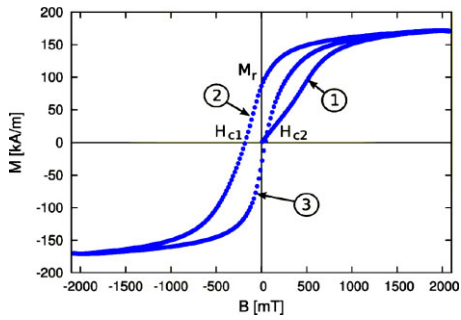

Figure 6.
Hysteresis loop of the magnetization of the sample.

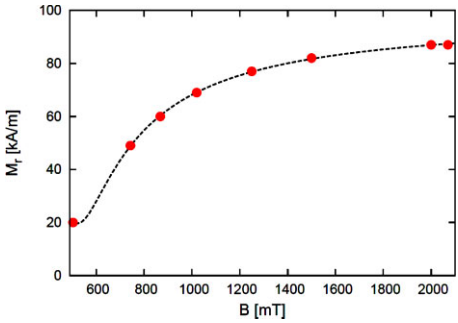

Figure 7.
Remanent magnetization of the MSE sample. The dotted line serves as a guide for eye.

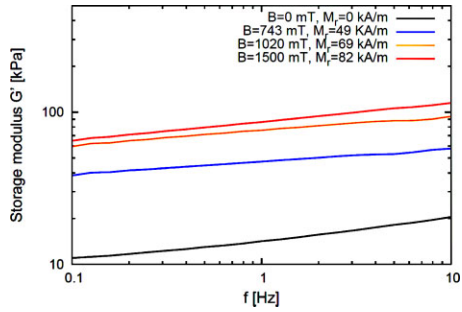

Figure 8.
Storage modulus of the sample as a function of an oscillation frequency at different remanent magnetizations (amplitude 1%).

Measurement of the Shear Modulus

Measurements of the storage modulus have been performed with the Anton Paar Physica MCR301 rheometer using the plate-plate geometry (diameter of the plates $d = 20\,mm$). The force normal to the shear direction has been kept at the constant value of $F_n = 3N$ in all experiments to avoid the influence of the deviation in the sample's compression ratio. To eliminate the possible slip between the surfaces of the sample and the oscillating plate of the rheometer, the last one has been covered with a thin layer of the basic composite.

Dependences of the shear modulus of MSE on the frequency and amplitude of the oscillation for the samples magnetized in the magnetic fields with various flux densities are shown in Figures 8 and 9 respectively. Similar to the classical soft MSEs,[34] the shear modulus of the MSE with magnetic hard filler increases with the frequency (Figure 8), at least in the considered range. The shape of the observed curves is roughly the same, i.e. the relative change of the modulus has a weak dependence on the sample magnetization.

Otherwise, the increase of the shear amplitude (Figure 9) results in the decrease of the sample modulus and the relative change of the modulus depends on the magnetization of the sample in the whole range of the used

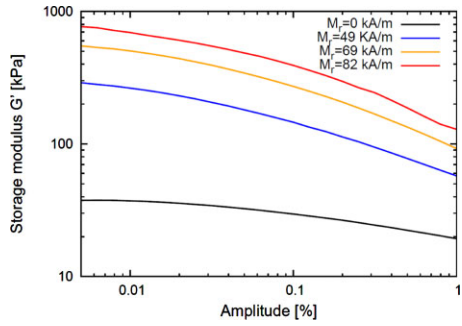

Figure 9.
Storage modulus of the sample as a function of a deformation amplitude at different remanent magnetizations (oscillation frequency 10 Hz).

shear amplitudes. This dependence tends to the linear one for the small amplitudes.

Qualitatively observed effects can be explained by the particles interaction and structure's formation induced by the sample magnetization.

Discussion

Predictions for the static shear modulus G, obtained in the frame of the microscopic theory can be compared with experimental results presented in the previous section. By doing this we assume that the values of storage modulus G' measured at sufficiently low frequencies ($f \leq 10Hz$) can be considered as a good representative of the static shear modulus G. Further we will use experimental

data for the storage modulus G' measured at frequency $f = 10Hz$ and at two amplitudes: $\gamma = 0.005\%$ and $\gamma = 1\%$. These experimental data are presented in Table 1 and shown in Figure 10 by data points.

To provide a good fit of the experimental data, let us look first at the equation (19) for the shear modulus G. One clearly sees that at small values of $\mathbf{M}_r$, $G(\mathbf{M}_r)$ can be approximately described by a parabolic function of $\mathbf{M}_r$:

$$G \cong G_0 + CM_r^2, \tag{21}$$

where the constant C is given by:

$$C = \frac{\mu_0}{4\pi} f_3(\alpha, \lambda_{eq}). \tag{22}$$

Parabola fit of the experimental data for G' by using equation (21) (lines in Figure 10) gives two values of C: $C = (160 \pm 5) \times 10^{-7} N/A^2$ and $C = (1082 \pm 12) \times 10^{-7} N/A^2$ for amplitudes $\gamma = 1\%$ and $\gamma = 0.005\%$, respectively. Note, that during fit procedure the parameter G_0 was fixed and equal to the material parameter at $\mathbf{M}_r = 0$.

Table 1.
Storage modulus G' vs the sample magnetization $\mathbf{M}_r$ as measured at frequency $f = 10Hz$.

$\mathbf{M}_r$ [kA/m]	0	49	69	82
G' [kPa], $\gamma = 0.005\%$	37.5	290	550	769
G' [kPa], $\gamma = 1\%$	19.3	57.5	92.4	129

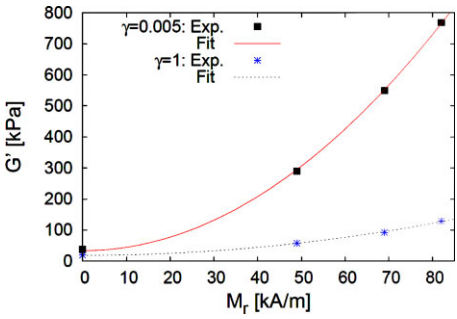

Figure 10.
Storage modulus G' vs the sample magnetization $\mathbf{M}_r$, obtained experimentally (symbols) and fitted (lines) with the help of equation (21).

Table 2.
Structure parameter α, estimated for the different magnetization $\mathbf{M}_r$ at two values of amplitude.

$\mathbf{M}_r$ [kA/m]	49	69	82
α, $\gamma = 0.005\%$	0.40	0.55	0.64
α, $\gamma = 1\%$	0.51	0.63	0.70

Knowing the value of C, we can calculate structure parameter α from equation (22). Note, that λ_{eq} itself depends on α and $\mathbf{M}_r$. As we shown in Figure 4 the values of equilibrium elongation λ_{eq} do not exceed 10% at $\alpha = 1$ and $\mathbf{M}_r = 82$ kA/m. However, we expect that magnetization of FeNdBr particles leads to the strong rearrangement of the particles into chains ($\alpha < 1$). As one can see from Figure 4 the values of equilibrium elongation λ_{eq} increase when α becomes less than 1. Thus, equation for α has to be solved at the different values of $\mathbf{M}_r$. The results are presented in Table 2:

From Table 2 we estimate the average values of α: $\alpha = 0.5 \pm 0.1$ and $\alpha = 0.6 \pm 0.1$ at the values of amplitude $\gamma = 0.005\%$ and $\gamma = 1\%$, respectively. One can see from these values of α, that the structure parameter α increases with the increase of amplitude of oscillatory deformation. This can be explained by the well-known Payne effect,[44] when increase of the deformation amplitude in a strain sweep experiment causes destruction of filler particles clusters in an elastomer matrix. Similar to the Payne effect, application of higher strains leads presumably to partial destruction of the chain-like structures of the magnetic particles, as result the particle distribution becoming more close to the isotropic one with $\alpha = 1$.

Conclusion

To summarize our study, we have presented a microscopical theory, which describes the mechanical behaviour of magneto-sensitive elastomers under a uniform external magnetic field. We used the regular rectangular lattice model for describing of the distribution of the magnetic particles inside the polymer matrix. The structure parameter

was introduced to describe different type of particles distributions such as isotropic, chain-like and plane-like. The magneto-induced deformation and the shear modulus were derived from the equation for the free energy and calculated as functions of the sample magnetization at different values of the structure parameter. It was shown that the shear modulus for the shear deformation perpendicular to the magnetic field increases for all spatial distributions of magnetic particles. Furthermore, we have compared our prediction for the shear modulus to the experimental data and found a good agreement, assuming formation of the chain-like structures of the magnetic particles under field application. Thus, the proposed microscopic model of MSEs is able to relate explicitly the microstructure of MSEs with their mechanical properties.

Appendix A

To derive an expression for the energy of magnetic particles in an external homogeneous magnetic field $\mathbf{H}_0$, consider the medium of the volume V and magnetic permeability of vacuum μ_0. Now let us introduce a magnetic particle of volume υ_1 and magnetic permeability μ into this medium. We assume that the particle is neutral and there are no external current densities. Affected by the field, the magnetic particle becomes polarized, forming a magnetic dipole and changing the field from $\mathbf{B}_0$ to $\mathbf{B}$ in all medium: $\mathbf{B} = \mathbf{B}_0 + \mathbf{B}_d$, where $\mathbf{B}_d$ is the dipole magnetic field:

$$B_d = \frac{\mu_0}{4\pi}\left[\frac{3(\mathbf{m}\cdot\mathbf{R})\mathbf{R}}{|\mathbf{R}|^5} - \frac{\mathbf{m}}{|\mathbf{R}|^3}\right], \tag{A.1}$$

created by the magnetic dipole $\mathbf{m}$ at the point $\mathbf{R}$. The change of the potential energy of such system after introduction of the magnetic particle is:

$$\Delta W = W - W_0 = -\frac{1}{2}\int_V \mathbf{BH}dV + \frac{1}{2}\int_V \mathbf{B}_0\mathbf{H}_0 dV, \tag{A.2}$$

where W is the potential energy of magnetic field $\mathbf{H}$, W_0 is the initial potential energy of magnetic field $\mathbf{H}_0$. We can rewrite the expression under integral in equation (A.2) as $\mathbf{BH} - \mathbf{B}_0\mathbf{H}_0 = \mathbf{BH} + \mathbf{BH}_0 + \mathbf{B}_0\mathbf{H} - \mathbf{BH}_0 - \mathbf{B}_0\mathbf{H} - \mathbf{B}_0\mathbf{H}_0$ and express the strength of the magnetic field $\mathbf{H}$ via the scalar potential φ as $\mathbf{H} = -\mathbf{grad}(\varphi)$. Thus, equation (A.2) takes a form:

$$\Delta W = \frac{1}{2}\int_V \mathbf{B}\mathbf{grad}(\varphi)dV - \frac{1}{2}\int_V \mathbf{BH}_0 dV - \frac{1}{2}\int_V \mathbf{B}_0\mathbf{grad}(\varphi)dV + \frac{1}{2}\int_V \mathbf{B}_0\mathbf{H}_0 dV. \tag{A.3}$$

Here we use the equality $\mathbf{B}_0\mathbf{H} - \mathbf{BH}_0 = 0$. Using the identity between the magnetic field and the scalar potential:

$$\mathrm{div}(\varphi\mathbf{F}) = \mathbf{grad}(\varphi)\cdot\mathbf{F} + \varphi\mathrm{div}(\mathbf{F}) \tag{A.4}$$

and the divergence theorem:

$$\int_V \mathrm{div}(\varphi\mathbf{F})\,dV = \oint (\varphi\mathbf{F}\cdot\mathbf{n})dS, \tag{A.5}$$

we have:

$$\Delta W = \frac{1}{2}\oint_S \varphi\mathbf{B}dS - \frac{1}{2}\int_V \mathbf{BH}_0 dV - \frac{1}{2}\oint_S \varphi\mathbf{B}_0 dS + \frac{1}{2}\int_V \mathbf{B}_0\mathbf{H}_0 dV. \tag{A.6}$$

Now, we choose the surfaces to be very far from the particle, so that $\mathbf{B} = \mathbf{B}_0$ on these surfaces and we have:

$$\Delta W = -\frac{1}{2}\int_V \mathbf{BH}_0 dV + \frac{1}{2}\int_V \mathbf{B}_0\mathbf{H}_0 dV = -\frac{1}{2}\int_V \mu_0\mathbf{M}\mathbf{H}_0 dV = W_{d_1}^{B_0}. \tag{A.7}$$

where the term $W_{d_1}^{B_0}$ means the energy of interaction between the magnetic dipole $\mathbf{m}_1 = \mathbf{M}_1\upsilon_1$ with magnetization $\mathbf{M}_1$ and the field $\mathbf{B}_0$. Thus, the total energy of external magnetic field and polarizable particle reads as:

$$W = W_0 + W_{d_1}^{B_0}. \tag{A.8}$$

Let's place the second magnetic particle of volume v_2 and magnetic permeability μ into the magnetic field $\mathbf{B} = \mathbf{B}_0 + \mathbf{B}_{d1}$, which is the field (considered above) in the presence of one permeable particle. Introducing the second particle will change the field from $\mathbf{B}$ to $\mathbf{B}'$. Repeating the procedure described above, we can show that the change of the potential energy of the magnetic field is equal to the energy of interaction between the magnetic dipole $\mathbf{m}_2 = \mathbf{M}_2 v_2$ with magnetization $\mathbf{M}_2$ and the field $\mathbf{B}$:

$$\begin{aligned} \Delta W &= -\frac{1}{2}\int_V \mathbf{B}'\mathbf{H}dV + \frac{1}{2}\int_V \mathbf{B}\mathbf{H}dV \\ &= -\frac{1}{2}\int_V \mu_0 \mathbf{M}_2\mathbf{H}dV = W_{d_2}^B. \end{aligned} \tag{A.9}$$

Thus, the change of energy of the system upon introducing two polarizable particles into external magnetic field $\mathbf{B}_0$ has a form:

$$\Delta W = W_{d_1}^{B_0} + W_{d_2}^B = W_{d_1}^{B_0} + W_{d_2}^{B_0} + W_{d_1 d_2}, \tag{A.10}$$

where $W_{d_1 d_2}$ is the energy of dipole-dipole interactions between particles. In the case of many particle system it can be shown that the magnetic energy is a sum of the dipole-dipole interaction energies, $W_{d_i d_j}$, and the dipole-field interaction energies, $W_{d_i}^{B_0}$. Thus, the magnetic energy of magnetic particles in an external homogeneous magnetic field takes a form of equation (8).

Acknowledgments: This project is funded by the European Union and the Free State of Saxony. D.B. thanks G. Stepanov for the sample preparation.

[1] G. Filipcsei, I. Csetneki, A. Szilágyi, M. Zrínyi, *Advances in Polymer Science* **2007**, *206*, 137–189.
[2] C. Ruddy, E. Ahearne, G. Byrne, in: *The 24th International Manufacturing Conference*, Waterford, **2007**.
[3] X.-M. Dong, M. Yu, C.-R. Liao, W.-M. Chen, *Transactions of Nonferrous Metals Society of China* **2009**, *19*, s611–s615.
[4] G. Y. Zhou, Z. Y. Jiang, *Smart Materials and Structures* **2004**, *13*, 309–316.
[5] V. G. Kulichikhin, A. V. Semakov, V. V. Karbushev, N. A. Platé, S. J. Picken, *Polymer Science Series A* **2009**, *51 (11&12)*, 1303–1312.
[6] X. Guan, X. Dong, J. Ou, *Journal of Magnetism and Magnetic Materials* **2008**, *320*, 158–163.
[7] S. Bednarek, *Applied Physics A* **1999**, *68*, 63–67.
[8] E. Coquelle, G. Bossis, *Journal of Advanced Science* **2005**, *17(1&2)*, 132–138.
[9] J. E. Martin, R. A. Anderson, D. Read, G. Gulley, *Physical Review E* **2006**, *74*, 051507.
[10] S. Abramchuk, E. Kramarenko, G. Stepanov, L. V. Nikitin, G. Filipcsei, A. R. Khokhlov, M. Zrínyi, *Polymers for Advanced Technologies* **2007**, *18*(11), 883–890.
[11] G. V. Stepanov, S. S. Abramchuk, D. A. Grishin, L. V. Nikitin, E. Yu. Kramarenko, A. R. Khokhlov, *Polymer* **2007**, *48*, 488–495.
[12] M. R. Jolly, J. D. Carlson, B. C. Muñoz, *Smart Materials and Structures* **1996**, *5*, 607–614.
[13] Y. M. Shkel, D. J. Klingenberg, in: *Proceedings of the 7th International Conference on Electro-Rheological Fluids and Magneto-Reological Suspensions*, World Scientific Publishing - Singapore, **2000**.
[14] Yu. L. Raikher, O. V. Stolbov, *Technical Physics Letters* **2000**, *26*(2), 156–158.
[15] L. Borcea, O. Bruno, *Journal of the Mechanics and Physics of Solids* **2001**, *49*, 2877–2919.
[16] Yu. L. Raikher, O. V. Stolbov, *Journal of Magnetism and Magnetic Materials* **2003**, *258-259*, 477–479.
[17] Yu. L. Raikher, O. V. Stolbov, *Journal of Magnetism and Magnetic Materials* **2005**, *289*, 62–65.
[18] G. Diguet, E. Beaugnon, J. Y. Cavaillé, *Journal of Magnetism and Magnetic Materials* **2010**, *322*, 3337–3341.
[19] E. Coquelle, G. Bossis, D. Szabo, F. Giulieri, *Journal of Materials Science* **2006**, *41*, 5941–5953.
[20] G. V. Stepanov, D. Yu. Borin, Yu. L. Raikher, P. V. Melenev, N. S. Perov, *Journal of Physics: Condensed Matter* **2008**, *20*, 204121.
[21] Yu. L. Raikher, O. V. Stolbov, *Journal of Physics: Condensed Matter* **2008**, *20*, 204126.
[22] Yu. L. Raikher, O. V. Stolbov, *Vychyslitilnaja Mekhanika Sploshnykh Sred* **2009**, *2*(2), 85–95.
[23] M. R. Jolly, J. D. Carlson, B. C. Muñoz, T. A. Bullions, *Journal of Intelligent Material Systems and Structures* **1996**, *7*(6), 613–622.
[24] D. Ivaneyko, V. P. Toshchevikov, M. Saphiannikova, G. Heinrich, *Macromolecular Theory and Simulations* **2011**, *20*(6), 411–424.
[25] D. Ivaneyko, V. Toshchevikov, M. Saphiannikova, G. Heinrich, *Condensed Matter Physics* **2012**, *15*(3), 33601.
[26] C. Bellan, G. Bossis, *International Journal of Modern Physics B* **2002**, *16(17&18)*, 2447–22453.
[27] Z. Varga, G. Filipcsei, M. Zrínyi, *Polymer* **2006**, *47*, 227–233.
[28] T. Shiga, A. Okada, T. Kurauchi, *Journal of Applied Polymer Science* **1995**, *58*, 787–792.
[29] S. A. Demchuk, V. A. Kuzmin, *Journal of Engineering Physics and Thermophysics* **2002**, *75*(2), 396–400.

[30] M. Lokander, B. Stenberg, *Polymer Testing* **2003**, *22*, 245–251.
[31] H. X. Deng, X. L. Gong, *Journal of Intelligent Material Systems and Structures* **2007**, *18*, 1205.
[32] W.-Q. Jiang, J.-J. Yao, X.-L. Gong, L. Chen, *Chinese Journal of Chemical Physics* **2008**, *21*(1), 87–8792.
[33] J. Wu, X. Gong, L. Chen, H. Xia, Z. Hu, *Journal of Applied Polymer Science* **2009**, *114*, 901–910.
[34] H. Böse, R. Röder, *Journal of Physics: Conference Series* **2009**, *149*, 012090.
[35] A. Boczkowska, S. F. Awietjan, *Journal of Materials Science* **2009**, *44*, 4104–4111.
[36] A. V. Chertovich, G. V. Stepanov, E. Yu. Kramarenko, A. R. Khokhlov, *Macromolecular Materials and Engineering* **2010**, *295*(4), 336–341.
[37] I. A. Brigadnov, A. Dorfmann, *International Journal of Solids and Structures* **2003**, *40*, 4659–4674.
[38] L. C. Davis, *Journal of Applied Physics* **1999**, *85*, 3348–3351.
[39] Y.-S. Zhu, X.-L. Gong, H. Dang, X.-Z. Zhang, P.-Q. Zhang, *Chinese Journal of Chemical Physics* **2006**, *19*, 126–130.
[40] L. R. G. Treloar, "*The Physics of Rubber Elasticity*", Oxford University Press, USA **2005**, 322 pp.
[41] M. Doi, S. F. Edwards, "*The Theory of Polymer Dynamic*", Clarendon Press, Oxford **1986**, 391 pp.
[42] C. W. Macosko, "*Rheology: Principles, Measurements, and Applications*", Wiley-VCH, **1994**, 533 pp.
[43] G. Filipcsei, M. Zrínyi, *Journal of Physics: Condensed Matter* **2010**, *22*(27), 276001.
[44] T. A. Vilgis, G. Heinrich, M. Klüppel, "*Reinforcement of Polymer Nano-Composites: Theory, Experiments and Applecations*", Cambridge University Press, **2009**, 209 pp.

